

Delamination analysis of inhomogeneous viscoelastic beam of rectangular section subjected to torsion

Victor I. Rizov*

Department of Technical Mechanics, University of Architecture, Civil Engineering and Geodesy, 1 Chr. Smirnensky Blvd., 1046-Sofia, Bulgaria

(Received January 7, 2023, Revised February 15, 2023, Accepted February 23, 2023)

Abstract. This paper considers a delamination analysis of a statically undetermined inhomogeneous beam structure of rectangular section with viscoelastic behavior under torsion. The beam is built in at its two ends. The beam has two longitudinal inhomogeneous layers with a delamination crack between them. A notch is made in the upper crack arm. The external torsion moment applied on the beam is a function of time. Under these conditions, the beam has one degree of indeterminacy. In order to derive the strain energy release rate, first, the static indeterminacy is resolved. Then the strain energy release rate is obtained by analyzing the balance of the energy with considering the viscoelastic behavior. The strain energy release rate is found also by analyzing the compliance of the beam for check-up. Solution of the strain energy release rate in a beam without a notch in the upper crack arm is derived too. In this case, the beam has two degrees of static indeterminacy (the torsion moment in the upper crack arm is treated as an additional internal redundant unknown). A parametric investigation of the strain energy release rate is carried-out.

Keywords: delamination; inhomogeneous beam structure; rectangular section; torsion moment; viscoelastic material

1. Introduction

Continuously inhomogeneous materials are a wide range of structural materials whose properties vary smoothly in the solid. The fact that the properties (elastic, viscoelastic, thermoelastic, etc.) are smooth functions of one or more coordinates makes the analysis of the mechanical behavior of various structural members and components built-up of continuously inhomogeneous materials more difficult in comparison with their homogeneous counterparts. Typical examples of continuously inhomogeneous materials are the functionally graded structural materials (Antonella Sola *et al.* 2016, Avcar and Mohammed 2018, Butcher *et al.* 1999, Gasik 2010, Han *et al.* 2001, Hedia *et al.* 2014, Hirai and Chen 1999, Mahamood and Akinlabi 2017). A functionally graded material is an inhomogeneous solid continuum that combines two or more constituent materials. During manufacturing, the constituent materials are continuously mixed. The microstructure and the ratio of constituent materials change smoothly along one or more

*Corresponding author, Professor, E-mail: V_RIZOV_FHE@UACG.BG

directions in the solid (Çallioglu *et al.* 2011, Çallioglu *et al.* 2015, Demir *et al.* 2013, El-Galy *et al.* 2019, Rabenda 2015, Rabenda and Michalak 2015, Rabenda 2016, Saiyathibrahim *et al.* 2016, Shrikantha and Gangadharan 2014, Wu *et al.* 2014). There are technologies for manufacturing of functionally graded materials which allow for tailoring of microstructure and material properties in order to obtain a desired profile of variation of the properties in a structural member or a component of engineering mechanism or device (Markworth *et al.* 1995, Miyamoto *et al.* 1999, Nemat-Allal *et al.* 2011, Sofiyev and Avcar 2010, Sofiyev *et al.* 2012, Toudehdeghghan *et al.* 2017, Uslu Uysal 2016). Therefore, it is not surprising that the wide application of functionally graded materials, especially in recent decades, contributes significantly for the advance in such key areas of the modern engineering as aeronautics, nuclear energetics, car industry, microelectronics, etc.

Analyzing of various fracture problems in continuously inhomogeneous (functionally graded) structural members and components under different loading conditions plays an important role in process of design of engineering structures in view of guaranteeing of their strength, stability, integrity, reliable functioning and economic efficiency (Dolgov 2005, Dolgov 2016). Lapses and negligence in assessing of fracture behavior may have heavy consequences for the safety and durability of the structure including catastrophic collapse.

This paper aims to analyze the delamination in an inhomogeneous statically undetermined beam structure of rectangular section loaded in torsion. The beam is made of two longitudinal inhomogeneous layers. The delamination is between layers. The beam considered has viscoelastic behaviour under external torsion moment that increases with time. Taking into account the viscoelastic behaviour is of great importance since very often engineering structures exhibit such behaviour under loading that is a function of time. The need of this paper follows from the fact that previous studies are concerned mainly with delamination analyses of inhomogeneous beams with circular cross-section subjected to pure torsion (Rizov 2018, Rizov 2020, Rizov 2020a, Rizov 2021, Rizov and Altenbach 2022). Delamination of inhomogeneous beams of rectangular cross-section under torsion also has been analyzed recently (Rizov 2022). However, the analysis presented in (Rizov 2022) deals with delamination of a statically determined cantilever beam. Due to the widespread application of statically undetermined beams in various engineering structures, the present paper is focused on delamination analysis of a beam that is built in at its two ends. In the present paper, solutions of the strain energy release rate are derived for two statically undetermined beam configurations under torsion (with and without a notch in the upper crack arm). The compliance method is applied in order to check the solutions. A parametric investigation is performed by using the solutions obtained.

2. Delaminated inhomogeneous beam built in at its two ends

The viscoelastic beam structure in Fig. 1 is under consideration in this paper. The section of the beam is a rectangle of width, b , and thickness, h . The beam length is designated by l . The beam is made of two adhesively bonded longitudinal layers. The thickness of the upper and lower layer is designated by h_1 and h_2 , respectively. A delamination crack of length, $a_1 + a_2$, is located between layers as shown in Fig. 1. A notch of depth, h_1 , is made in the upper crack arm. As a result of this, the upper crack arm is free of stresses. The beam is clamped in its two ends. An external torsion moment, T , is applied in section, B_4 , of the beam. The variation of T with time, t , is written as

$$T = v_T t, \quad (1)$$

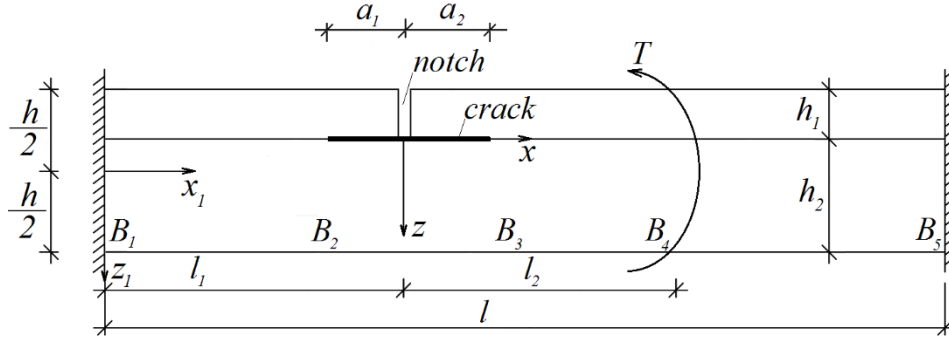


Fig. 1 Inhomogeneous viscoelastic beam with a delamination loaded in torsion

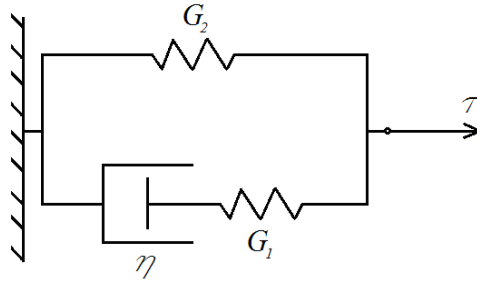


Fig. 2 Viscoelastic mechanical model

where v_t is a parameter that controls the torsion moment. Under torsion, the beam in Fig. 1 is a statically undetermined structure with one degree of indeterminacy.

The viscoelastic behaviour of the upper layer of the beam is analyzed by using the viscoelastic mechanical model shown in Fig. 2.

The model is under shear stress, τ , that varies with time according to the following law

$$\tau = v_\tau t, \quad (2)$$

where the parameter, v_τ , controls the shear stress. The stress-strain-time relationship of the model in Fig. 2 is found by solving its differential equation of equilibrium. The result is

$$\gamma(t) = \beta_2 \left(1 - e^{-\frac{G_2 t}{\beta_1}} \right) + \beta_3 t, \quad (3)$$

where

$$\beta_1 = \eta + \eta \frac{G_2}{G_1}, \quad (4)$$

$$\beta_2 = \frac{1}{G_2} \left(\frac{v_\tau \eta}{G_1} - \frac{v_\tau \beta_1}{G_2} \right), \quad (5)$$

$$\beta_3 = \frac{v_\tau}{G_2}. \quad (6)$$

In formulae (3), (4), (5) and (6), G_1 and G_2 are the shear moduli of the two springs, η is the coefficient of viscosity of the dashpot in the model (Fig. 2).

The time-dependent shear modulus, G_* , of the upper layer is written as

$$G^* = \frac{\tau}{\gamma}. \quad (7)$$

By combining of (2), (3) and (7), one obtains

$$G^* = \left[\beta_{2r} \left(1 - e^{-\frac{G_2 t}{\beta_1}} \right) + \beta_{3r} \right]^{-1}, \quad (8)$$

where

$$\beta_{2r} = \frac{1}{t G_2} \left(\frac{\eta}{G_1} - \frac{\beta_1}{G_2} \right), \quad (9)$$

$$\beta_{3r} = \frac{1}{G_2}. \quad (10)$$

The viscoelastic behaviour of the lower layer of the beam is modelled also by applying relationship (3). For this purpose, G_1 , G_2 and η are replaced with G_{1L} , G_{2L} and η_L , respectively. Here, G_{1L} , G_{2L} and η_L are the shear moduli and the coefficient of viscosity of the viscoelastic model of the lower layer. The time-dependent shear modulus, G_{*L} , of the lower layer is found by replacing of G_1 , G_2 and η with G_{1L} , G_{2L} and η_L in (8). It should be mentioned that the time-dependent moduli, G^* and G_{*L} , are used in the delamination analysis developed in this paper.

The two layers of the beam exhibit continuous material inhomogeneity in longitudinal direction. The following laws are used for treating the distribution of the material properties in the upper layer along the beam length

$$G_1 = G_{1P} e^{g_1 \frac{x_1}{l}}, \quad (11)$$

$$G_2 = G_{2P} e^{g_2 \frac{x_1}{l}}, \quad (12)$$

$$\eta = \eta_P e^{g_3 \frac{x_1}{l}}, \quad (13)$$

where

$$0 \leq x_1 \leq l. \quad (14)$$

In formulae (11), (12), (13) and (14), x_1 is the longitudinal centroidal axis of the beam, G_{1P} , G_{2P} and η_P are the values of G_1 , G_2 and η at the left-hand end of the beam, g_1 , g_2 and g_3 are parameters which control the distribution of material properties.

The distribution of material properties in the lower layer is treated also by (11), (12) and (13). For this purpose, of G_1 , G_2 , η , g_1 , g_2 and g_3 are replaced with G_{1L} , G_{2L} , η_L , f_1 , f_2 and f_3 , respectively.

The strain energy release rate, G , for the delamination problem shown in Fig. 1 is derived by analyzing the balance of the energy. For this purpose, first, the static indeterminacy is resolved. The torsion moment, T_p , in the left-hand clamping is treated as redundant unknown. The static indeterminacy is resolved by using the theorem of Menabrea

$$\frac{\partial U^*}{\partial T_p} = 0, \quad (15)$$

where U is the strain energy in the beam. U is found as

$$U = U_1 + U_2 + U_3 + U_4, \quad (16)$$

where U_1 , U_2 , U_3 and U_4 are the strain energies in beam portion, $B_1 B_2$, in the lower crack arm and in beam portions, $B_3 B_4$ and $B_4 B_5$, respectively (Fig. 1). The analysis is carried-out in coordinate

system, xz (Fig. 1).

The strain energy in beam portion, B_1B_2 , is written as

$$U_1 = \int_{-l_1}^{-a_1} \frac{T_P^2}{2G^*D I} dx, \quad (17)$$

where l_1 is the length of this portion, $G^*D I$ is rigidity in torsion of the beam. $G^*D I$ is calculated as (Muskhelishvili 1996)

$$G^*D I = \frac{8}{3}(G^*h_1 + G^*L h_2) \left(\frac{b}{2}\right)^3 + \left(\frac{4}{\pi}\right)^5 \left(\frac{b}{2}\right)^4 \sum_{i=0}^{\infty} \left[\frac{G^{*2}ch(jh_2) + G^{*2}_L ch(jh_1)}{Q} - \frac{(G^{*2} + G^{*2}_L)ch(jh_1)ch(jh_2)}{Q} \right] - \left(\frac{4}{\pi}\right)^5 \left(\frac{b}{2}\right)^4 G^*G^*L \sum_{i=0}^{\infty} \left\{ \frac{ch(jh_1) + ch(jh_2)}{Q} - \frac{ch[h(h_1 - h_2)] - 1}{Q} \right\} \quad (18)$$

where

$$Q = (2i + 1)^5 [G^*ch(jh_2)sh(jh_1) + G^*L ch(jh_1)sh(jh_2)], \quad (19)$$

$$j = \frac{(2i+1)\pi}{b}. \quad (20)$$

It should be noted that $G^*D I$ is a function of time and x since the shear moduli, G^* and G^*L , depend on time and x .

The strain energy in the lower crack arm is derived as

$$U_2 = \int_{-a_1}^{a_2} \frac{T_P^2}{2G^*L I_2} dx, \quad (21)$$

where the moment of inertia, I_2 , of this crack arm is determined as (Muskhelishvili 1996)

$$I_2 = \frac{h_2 b^3}{3} - \left(\frac{4}{\pi}\right)^5 \left(\frac{b}{2}\right)^4 \sum_{i=1}^{\infty} \frac{th(jh_2)}{(2i+1)^5}. \quad (22)$$

The strain energies in the beam portions, B_3B_4 and B_4B_5 , are derived as

$$U_3 = \int_{a_2}^{l_2} \frac{T_P^2}{2G^*D I} dx \quad (23)$$

and

$$U_4 = \int_{l_2}^{l-l_1} \frac{(T_P - T)^2}{2G^*D I} dx, \quad (24)$$

respectively.

After substituting of the strain energy, U , in (15), the equation is solved with respect to T_P .

By analyzing the balance of the energy, the strain energy release rate for increase of delamination at the left-hand delamination tip (at section, B_2 , of the beam) is found as

$$G = \frac{1}{b} \left(T \frac{\partial \phi}{\partial a_1} - \frac{\partial U}{\partial a_1} \right), \quad (25)$$

where ϕ is the angle of twist of section, B_4 (Fig. 1). In order to derive the strain energy release rate by using (25), the angle of twist has to be presented as a function of the crack length. For this purpose, the integrals of Maxwell-Mohr applied for calculating of ϕ in the statically undetermined system are written in the form

$$\phi = \int_{-l_1}^{-a_1} \frac{T_P}{G^*D I} \frac{T_P}{T} dx + \int_{-a_1}^{a_2} \frac{T_P}{G^*L I_2} \frac{T_P}{T} dx + \int_{a_2}^{l_2} \frac{T_P}{G^*D I} \frac{T_P}{T} dx + \int_{l_2}^{l-l_1} \frac{T_P - T}{G^*D I} \frac{T_P - T}{T} dx, \quad (26)$$

where T_p/T and $(T_p - T)/T$ are the torsion moments in the beam portions induced by the unit loading for determination of the angle of twist.

By combining of (16), (25) and (26), one obtains

$$G = \frac{1}{2b} \left(-\frac{T_p^2}{G^*_{D^*}I} + \frac{T_p^2}{G^*_{L}I_2} \right), \quad (27)$$

where the material properties involved in $G^*_{D^*}I$ and $G^*_{L}I_2$ are found at $x_1 = l_1 - a_1$. The strain energy release rate can be calculated by using (27) at various values of time.

In order to verify (27), the strain energy release rate is derived also by analyzing the compliance, C , of the beam. For this purpose, the compliance is determined as

$$C = \frac{\phi}{T}. \quad (28)$$

The strain energy release rate is written as

$$G = \frac{T^2}{2b} \frac{dC}{da_1}. \quad (29)$$

By combining of (26), (28) and (29), one obtains

$$G = \frac{1}{2b} \left(-\frac{T_p^2}{G^*_{D^*}I} + \frac{T_p^2}{G^*_{L}I_2} \right), \quad (30)$$

where the material properties are calculated at $x_1 = l_1 - a_1$. The fact that (30) is match of (27) proves the correctness of the present analysis.

The strain energy release rate for increase of delamination at the right-hand delamination tip (located in section, B_3 , of the beam (Fig. 1)) found by analyzing the balance of the energy has the following form

$$G = \frac{1}{b} \left(T \frac{\partial \phi}{\partial a_2} - \frac{\partial U}{\partial a_2} \right). \quad (31)$$

By using of (16), (26) and (31), one derives

$$G = \frac{1}{2b} \left(\frac{T_p^2}{G^*_{L}I_2} - \frac{T_p^2}{G^*_{D^*}I} \right), \quad (32)$$

where the material properties involved in $G^*_{D^*}I$ and $G^*_{L}I_2$ are found at $x_1 = l_1 + a_2$.

By analyzing the compliance of the beam, the strain energy release rate for increase of delamination at the right-hand delamination tip is written as

$$G = \frac{T^2}{2b} \frac{dC}{da_2}. \quad (33)$$

By substituting of (26) and (26) in (33), one obtains

$$G = \frac{1}{2b} \left(\frac{T_p^2}{G^*_{L}I_2} - \frac{T_p^2}{G^*_{D^*}I} \right). \quad (34)$$

The material properties in (34) are found at $x_1 = l_1 + a_2$. Expression (34) coincides with (32) which proves the correctness of the analysis.

The strain energy release rate is obtained also assuming that there is not a notch in the upper crack arm in the beam in Fig. 1. In this case, the beam has two degrees of indeterminacy. The torsion moments in the left-hand clamping and in the upper crack arm, T_p and T_1 , are treated as redundant unknowns. The static indeterminacy is resolved by using the theorem of Menabrea

$$\frac{\partial U}{\partial T_p} = 0, \quad (35)$$

$$\frac{\partial U}{\partial T_1} = 0. \quad (36)$$

The strain energy in the beam is found as

$$U = \int_{-l_1}^{a_1} \frac{T_P^2}{2G^*_{DI}} dx + \int_{-a_1}^{a_2} \frac{T_1^2}{2G^*_{I_1}} dx + \int_{-a_1}^{a_2} \frac{T_2^2}{2G^*_{LI_2}} dx + \int_{a_2}^{l_2} \frac{T_P^2}{G^*_{DI}} dx + \int_{l_2}^{l-l_1} \frac{(T_P-T)^2}{G^*_{DI}} dx, \quad (37)$$

where T_2 is the torsion moment in the lower crack arm. The moment of inertia, I_1 , of the upper crack arm is determined as (Muskhelishvili 1996)

$$I_1 = \frac{h_1 b^3}{3} - \left(\frac{4}{\pi}\right)^5 \left(\frac{b}{2}\right)^4 \sum_{i=1}^{\infty} \frac{th(jh_1)}{(2i+1)^5}. \quad (38)$$

By using the equation of equilibrium of the torsion moments in the upper and lower crack arms, one derives

$$T_2 = T_P - T_1. \quad (39)$$

By combining of (37) and (39), one obtains the following expression for the strain energy

$$U = \int_{-l_1}^{a_1} \frac{T_P^2}{2G^*_{DI}} dx + \int_{-a_1}^{a_2} \frac{T_1^2}{2G^*_{I_1}} dx + \int_{-a_1}^{a_2} \frac{(T_P-T_1)^2}{2G^*_{LI_2}} dx + \int_{a_2}^{l_2} \frac{T_P^2}{G^*_{DI}} dx + \int_{l_2}^{l-l_1} \frac{(T_P-T)^2}{G^*_{DI}} dx. \quad (40)$$

After substituting of the strain energy in (35) and (36), the two equations are solved with respect to T_P and T_1 .

By analyzing the energy balance, the strain energy release rate for increase of delamination at the left-hand delamination tip is derived as

$$G = \frac{1}{2b} \left(-\frac{T_P^2}{G^*_{DI}} + \frac{(T_P-T_1)^2}{G^*_{LI_2}} + \frac{T_1^2}{G^*_{I_1}} \right), \quad (41)$$

where the material properties involved in G^*_{DI} , $G^*_{I_1}$ and $G^*_{LI_2}$ are found at $x_1 = l_1 - a_1$.

By applying the compliance method, the strain energy release rate for increase of delamination at the left-hand delamination tip is found as

$$G = \frac{1}{2b} \left(-\frac{T_P^2}{G^*_{DI}} + \frac{(T_P-T_1)^2}{G^*_{LI_2}} + \frac{T_1^2}{G^*_{I_1}} \right). \quad (42)$$

Here, the material properties in G^*_{DI} , $G^*_{I_1}$ and $G^*_{LI_2}$ are determined at $x_1 = l_1 - a_1$. Formulas (42) and (41) are identical. This fact is a control of the solution of the strain energy release rate for increase of delamination at the left-hand delamination tip in the beam configuration without notch in the upper crack arm.

The analysis of the balance of the energy yields the following expression for the strain energy release rate at increase of the delamination at the right-hand delamination tip in the beam without a notch in the upper crack arm

$$G = \frac{1}{2b} \left(\frac{T_1^2}{G^*_{I_1}} + \frac{(T_P-T_1)^2}{G^*_{LI_2}} - \frac{T_P^2}{G^*_{DI}} \right). \quad (43)$$

In (43), the material properties involved in G^*_{DI} , $G^*_{I_1}$ and $G^*_{LI_2}$ are found at $x_1 = l_1 + a_2$.

By using the compliance method, one derives

$$G = \frac{1}{2b} \left(\frac{T_1^2}{G^*_{I_1}} + \frac{(T_P-T_1)^2}{G^*_{LI_2}} - \frac{T_P^2}{G^*_{DI}} \right), \quad (44)$$

where the material properties are obtained at $x_1 = l_1 + a_2$. Formula (44) is match of (43) which is a check-up of the solution of the strain energy release rate for increase of the delamination at the

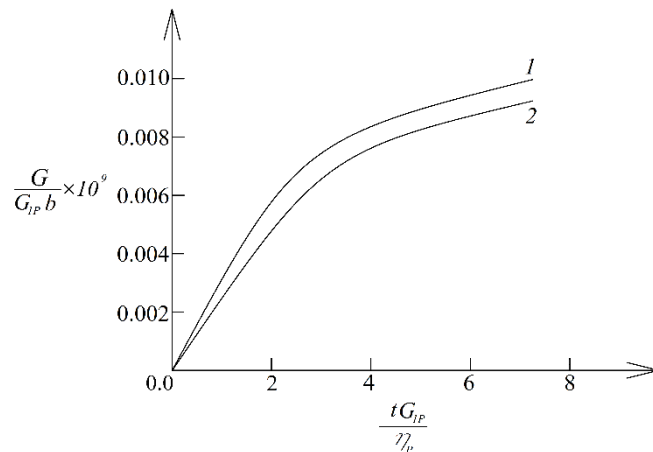


Fig. 3 The strain energy release rate displayed as a function of time (curve 1-for beam configuration with notch in the upper crack arm and curve 2-at beam configuration without notch)

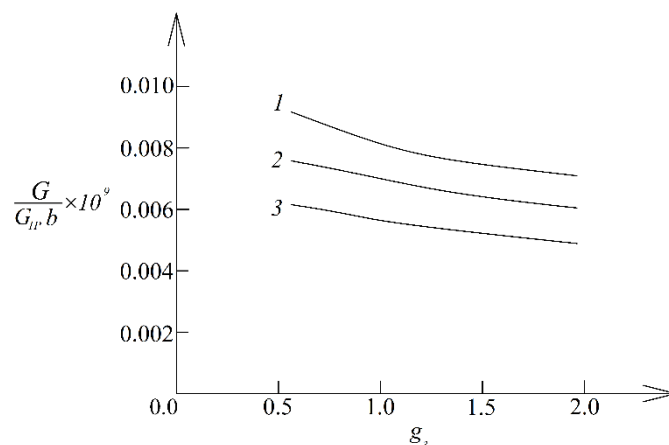


Fig. 4 The strain energy release rate displayed as a function of g_3 (curve 1-at $g_1 = 0.5$, curve 2-at $g_1 = 1.0$ and curve 3-at $g_1 = 2.0$)

right-hand delamination tip in the beam without a notch in the upper crack arm.

3. Parametric investigation

A parametric investigation of the strain energy release rate for the delamination problem in Fig. 1 is carried-out. The following data are used in the parametric investigation: $b = 0.030$ m, $h = 0.040$ m, $l = 0.650$ m, $l_1 = 0.250$ m, $l_2 = 0.300$ m and $v_T = 0.8 \times 10^{-5}$ Nm/s.

The evolution of the strain energy release rate with time is displayed in Fig. 3 for both beam configurations (with and without notch in the upper crack arm). The solution of the strain energy release rate at increase of delamination at the left-hand delamination tip (in section, B_2 , of the beam) is used. The strain energy release rate and the time in Fig. 3 are presented in non-

dimensional form by using the formulae $G_N = G/(G_{1P}b)$ and $t_N = tG_{1P}/\eta_P$, respectively. One can observe in Fig. 3 that the strain energy release rate for the beam configuration with notch in the upper crack arm is higher than that in the beam configuration without notch (this finding can be explained by the circumstance that the beam configuration with notch in the upper crack arm is more deformable in comparison to the beam configuration without notch).

The influence of parameters, g_1 and g_3 , on the strain energy release rate is analyzed.

The results of this analysis are displayed in Fig. 4 where the strain energy release rate in non-dimensional form is plotted against g_3 for three values of the parameter, g_1 .

The curves in Fig. 4 indicate that the strain energy release rate reduces when g_1 increases.

It can be observed in Fig. 4 that increase of g_3 causes also reduction of the strain energy release rate. This behavior is a consequence of the fact that the beam rigidity increases when parameters, g_1 and g_3 , increase.

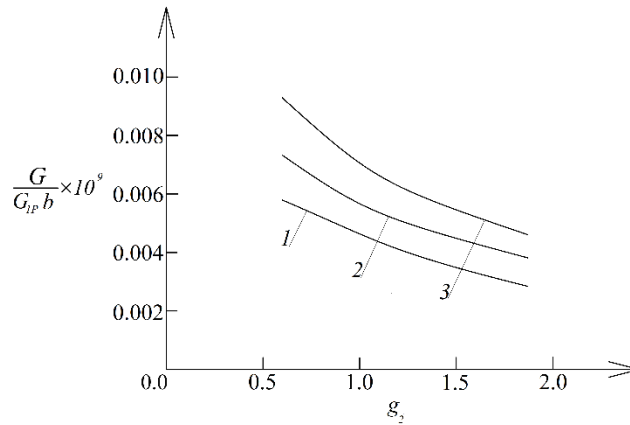


Fig. 5 The strain energy release rate displayed as a function of g_2 (curve 1 - at $h_1/h = 0.2$, curve 2 - at $h_1/h = 0.4$ and curve 3 - at $h_1/h = 0.6$)

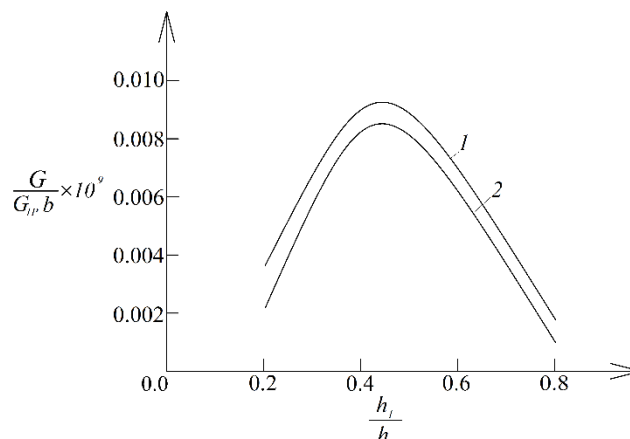


Fig. 6 The strain energy release rate displayed as a function of h_1/h ratio for the beam configuration without notch in the upper crack arm (curve 1-at increase of the delamination at the left-hand delamination tip and curve 2-at increase of the delamination at the right-hand delamination tip)

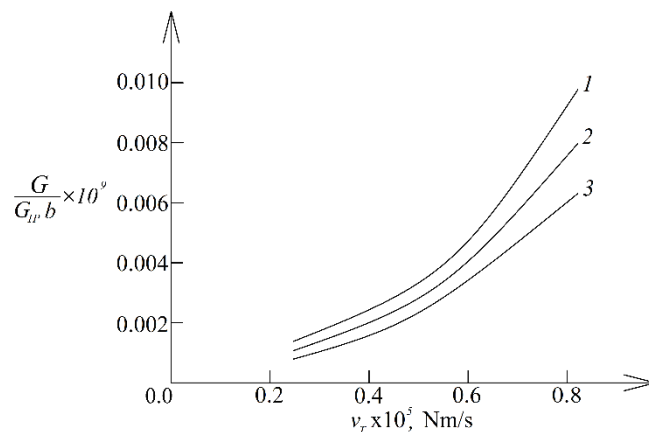


Fig. 7 The strain energy release rate displayed as a function of v_T (curve 1 - at $h/b = 1.3$, curve 2 - at $h/b = 1.5$ and curve 3 - at $h/b = 1.7$)

The effect of parameter, g_2 , on the strain energy release rate is analyzed too.

The change of the strain energy release rate with increase of g_2 at three h_1/h ratios is displayed in Fig. 5 for the beam configuration with notch in the upper crack arm. Here, again the strain energy release rate is presented in non-dimensional form. The inspection of curves in Fig. 5 reveals that when g_2 increases, the strain energy release rate reduces. One can observe in Fig. 5 that increase of h_1/h ratio generates increase of the strain energy release rate. This is due to fact that the rigidity of the lower crack arm decreases (the upper crack arm is free of stresses because of the notch).

The influence of h_1/h ratio on the strain energy release rate is analyzed also for the beam configuration without notch in the upper crack arm. The variation of the non-dimensional strain energy release rate with increase of h_1/h ratio is displayed in Fig. 6. It is evident from Fig. 6 that the strain energy release rate has maximum when the crack is near the mid-plane of the beam structure. Also, one can observe in Fig. 6 that the strain energy release rate at increase of the delamination at the left-hand delamination tip is higher than that at increase of the delamination at the right-hand delamination tip (in section, B_3 , of the beam). This is due to the fact that the values of material properties increase from the left-hand end of the beam towards the right-hand end of the beam.

The effects of the parameter, v_T , and h/b ratio on the strain energy release rate are illustrated in Fig. 7 where the dependency of the non-dimensional strain energy release rate on the parameter, v_T , is shown at three values of h/b ratio. It can be observed in Fig. 7 that increase of v_T induces increase of the strain energy release rate. When h/b ratio increases, the strain energy release rate reduces (Fig. 7) which is explained by increase of the beam rigidity.

4. Conclusions

An analysis of the strain energy release rate for a delamination crack in a statically undetermined viscoelastic beam of rectangular section loaded in torsion is carried-out. The beam is made of two longitudinal layers which are inhomogenous along the beam length. The delamination

is located between the layers. A vertical notch is made in the upper crack arm. The strain energy is obtained by analyzing the energy balance. The compliance method is applied for check-up. The strain energy release rate is found also for the beam configuration without notch in the upper crack arm. The parametric investigation reveals that the strain energy release rate reduces when parameters, g_1 , g_2 and g_3 , increase. The increase of h/b ratio generates also reduction of the strain energy release rate. The analysis indicates that when v_T increases, the strain energy release rate increases too. The increase of h_1/h ratio induces increase of the strain energy release rate for the beam configuration with notch in the upper crack arm. However, the strain energy release rate has maximum when the crack is near the mid-plane in the beam without notch in the upper crack arm. It is found also that the strain energy release rate at increase of delamination at the left-hand delamination tip is higher in comparison with that at increase of delamination at the right-hand delamination tip. It should be mentioned that besides for fracture in layered inhomogeneous beam configurations, this study can also be applied in analyzing the fracture behavior of laminated glass structures (Galic *et al.* 2022, Grozdanic *et al.* 2021) where the interlayer exhibits viscoelastic behavior and one of the glass panels is damaged (cracks through section).

References

- Avcar, M. and Mohammed, W.K.M. (2018), "Free vibration of functionally graded beams resting on Winkler-Pasternak foundation", *Arab. J. Geosci.*, **11**, 232. <https://doi.org/10.1007/s12517-018-3579-2>.
- Butcher, R.J., Rousseau, C.E. and Tippur, H.V. (1999), "A functionally graded particulate composite: Measurements and failure analysis", *Acta Mater.*, **47**(2), 259-268. [https://doi.org/10.1016/S1359-6454\(98\)00305-X](https://doi.org/10.1016/S1359-6454(98)00305-X).
- Çallioğlu, H., Sayer, M. and Demir, E. (2011), "Stress analysis of functionally graded discs under mechanical and thermal loads", *Ind. J. Eng. Mater. Sci.*, **18**(2), 111-118.
- Çallioğlu, H., Sayer, M. and Demir, E. (2015), "Elastic-plastic stress analysis of rotating functionally graded discs", *Thin Wall. Struct.*, **94**, 38-44. <https://doi.org/10.1016/j.tws.2015.03.016>.
- Demir, E., Çallioğlu, H. and Sayer, M. (2013), "Free vibration of symmetric FG sandwich Timoshenko beam with simply supported edges", *Ind. J. Eng. Mater. Sci.*, **20**(6), 515-521.
- Dolgov, N.A. (2005), "Determination of stresses in a two-layer coating", *Strength Mater.*, **37**(2), 422-431. <https://doi.org/10.1007/s11223-005-0053-7>.
- Dolgov, N.A. (2016), "analytical methods to determine the stress state in the substrate-coating system under mechanical loads", *Strength Mater.*, **48**(1), 658-667. <https://doi.org/10.1007/s11223-016-9809-5>.
- El-Galy, I.M., Saleh, B.I. and Ahmed, M.H. (2019), "Functionally graded materials classifications and development trends from industrial point of view", *SN Appl. Sci.*, **1**, 1378. <https://doi.org/10.1007/s42452-019-1413-4>.
- Galic, M., Grozdanic, G., Divic, V. and Marovic, P. (2022), "Parametric analyses of the influence of temperature, load duration, and interlayer thickness on a laminated glass structure exposed to out-of-plane loading", *Crystal.*, **12**(6), 838. <https://doi.org/10.3390/cryst12060838>.
- Gasik, M.M. (2010), "Functionally graded materials: bulk processing techniques", *Int. J. Mater. Prod. Technol.*, **39**(1-2), 20-29. <https://doi.org/10.1504/IJMPT.2010.034257>.
- Grozdanic, G., Galic, M. and Marovic, P. (2021), "Some aspects of the analyses of glass structures exposed to impact load", *Couple. Syst. Mech.*, **10**(6), 475-490. <https://doi.org/10.12989/csm.2021.10.6.475>.
- Han, X., Xu, Y.G. and Lam, K.Y. (2001), "Material characterization of functionally graded material by means of elastic waves and a progressive-learning neural network", *Compos. Sci. Technol.*, **61**(10), 1401-1411. [https://doi.org/10.1016/S0266-3538\(01\)00033-1](https://doi.org/10.1016/S0266-3538(01)00033-1).
- Hedia, H.S., Aldousari, S.M., Abdellatif, A.K. and Fouda, N.A. (2014), "New design of cemented stem using functionally graded materials (FGM)", *Biomed. Mater. Eng.*, **24**(3), 1575-1588.

- <https://doi.org/10.3233/BME-140962>.
- Hirai, T. and Chen, L. (1999), "Recent and prospective development of functionally graded materials in Japan", *Mater. Sci. Forum*, **308-311**(4), 509-514. <https://doi.org/10.4028/www.scientific.net/MSF.308-311.509>.
- Mahamood, R.M. and Akinlabi, E.T. (2017), *Functionally Graded Materials*, Springer.
- Markworth, A.J., Ramesh, K.S. and Parks, Jr. W.P. (1995), "Review: Modeling studies applied to functionally graded materials", *J. Mater. Sci.*, **30**(3), 2183-2193. <https://doi.org/10.1007/BF01184560>.
- Miyamoto, Y., Kaysser, W.A., Rabin, B.H., Kawasaki, A. and Ford, R.G. (1999), *Functionally Graded Materials: Design, Processing and Applications*, Kluwer Academic Publishers, Dordrecht/London/Boston.
- Muskhelishvili, N. (1996), *Some Basic Problems in the Mathematical Theory of Elasticity*, Science.
- Nemat-Allal, M.M., Ata, M.H., Bayoumi, M.R. and Khair-Eldeen, W. (2011), "Powder metallurgical fabrication and microstructural investigations of Aluminum/Steel functionally graded material", *Mater. Sci. Appl.*, **2**(5), 1708-1718. <https://doi.org/10.4236/msa.2011.212228>.
- Rabenda, M. (2015), "Analysis of non-stationary heat transfer in a hollow cylinder with functionally graded material properties performed by different research methods", *Eng. Transac.*, **63**, 329-339.
- Rabenda, M. (2016), "The analysis of the impact of different shape functions in tolerance modeling on natural vibrations of the rectangular plate with dense system of the ribs in two directions", *Vib. Phys. Syst.*, **27**, 301-308.
- Rabenda, M. and Michalak, B. (2015), "Natural vibrations of prestressed thin functionally graded plates with dense system of ribs in two directions", *Compos. Struct.*, **133**, 1016-1023. <https://doi.org/10.1016/j.compstruct.2015.08.026>.
- Rizov, V. and Altenbach, H. (2022), "Multi-layered non-linear viscoelastic beams subjected to torsion at a constant speed: A delamination analysis", *Eng. Trans.*, **70**, 53-66. <https://doi.org/10.24423/EngTrans.1720.20220303>.
- Rizov, V.I. (2018), "Non-linear fracture in bi-directional graded shafts in torsion", *Multidisc. Model. Mater. Struct.*, **14**, 387-399. <https://doi.org/10.1108/MMMS-12-2017-0163>.
- Rizov, V.I. (2020), "Longitudinal fracture analysis of inhomogeneous beams with continuously changing radius of cross-section along the beam length", *Strength Fract. Complex.*, **13**, 31-43. <https://doi.org/10.3233/SFC-200250>.
- Rizov, V.I. (2020a), "Longitudinal fracture analysis of continuously inhomogeneous beam in torsion with stress relaxation", *Struct. Integr. Procedia*, **28**, 1212-122. <https://doi.org/10.1016/j.prostr.2020.11.103>.
- Rizov, V.I. (2021), "Delamination analysis of multilayered beams exhibiting creep under torsion", *Couple. Syst. Mech.*, **10**, 317-331. <https://doi.org/10.12989/csm.2021.10.4.317>.
- Rizov, V.I. (2022), "Inhomogeneous beam structures of rectangular cross-section loaded in torsion: A delamination study with considering creep", *Procedia Struct. Integr.*, **41**, 94-102. <https://doi.org/10.1016/j.prostr.2022.05.012>.
- Saiyathibrahim, A., Subramaniyan, R. and Dhanapl, P. (2016), "Centrifugally cast functionally graded materials-Review", *International Conference on Systems, Science, Control, Communications, Engineering and Technology*, 68-73.
- Shrikantha Rao, S. and Gangadharan, K.V. (2014), "Functionally graded composite materials: An overview", *Procedia Mater. Sci.*, **5**(1), 1291-1299. <https://doi.org/10.1016/j.mspro.2014.07.442>.
- Sofiyev, A.H. and Avcar, M. (2010), "The stability of cylindrical shells containing an FGM layer subjected to axial load on the Pasternak foundation", *Eng.*, **2**, 228-236. <https://doi.org/10.4236/eng.2010.24033>.
- Sofiyev, A.H., Alizada, A.N., Akin, Ö. Valiyev, A., Avcar, M. and Adiguzel, S. (2012), "On the stability of FGM shells subjected to combined loads with different edge conditions and resting on elastic foundations", *Acta Mechanica*, **223**, 189-204. <https://doi.org/10.1007/s00707-011-0548-1>.
- Sola, A., Bellucci, D. and Cannillo, V. (2016), "Functionally graded materials for orthopedic applications-an update on design and manufacturing", *Biotechnol. Adv.*, **34**, 504-531. <https://doi.org/10.1016/j.biotechadv.2015.12.013>.
- Toudehdehghan, A., Lim, J.W., Foo, K.E., Ma'Arof, M.I.N. and Mathews, J. (2017), "A brief review of

- functionally graded materials”, *MATEC Web Conf.*, **131**, 03010. <https://doi.org/10.1051/mateconf/201713103010UTP-UMP>.
- Uslu Uysal, M. (2016), “Buckling behaviours of functionally graded polymeric thin-walled hemispherical shells”, *Steel Compos. Struct.*, **21**(1), 849-862. <https://doi.org/10.12989/scs.2016.21.4.849>.
- Wu, X.L., Jiang, P., Chen, L., Zhang, J.F., Yuan, F.P. and Zhu, Y.T. (2014), “Synergetic strengthening by gradient structure”, *Mater. Res. Lett.*, **2**(1), 185-191. <https://doi.org/10.1080/21663831.2014.935821>.

CC